Iron III Half Salen Catalysts for Atom Transfer Radical and Ring-Opening Polymerizations

ACS OMEGA

Article

Cite This: ACS Omega 2018, 3, 16945−16953

http://pubs.acs.org/journal/acsodf

Iron^{III} Half Salen Catalysts for Atom Transfer Radical and Ring-Opening Polymerizations

Eszter Fazekas, Gary S. Nichol, Jennifer A. Garden,* and Michael P. Shaver*

EaStCHEM School of Chemistry, University of Edinburgh, Edinburgh EH9 3FJ, U.K.

Supporting Information

ABSTRACT: A series of monometallic pentacoordinate Fe^{III} chloride complexes have been prepared and characterized by high-resolution mass spectrometry and elemental analysis. X-ray diffraction analysis showed that the bis-chelated Fe^{III} complexes bear distorted trigonal bipyramidal geometries. The air- and moisture-stable Fe^{III} complexes were screened as mediators in the reverse atom transfer radical polymerization (ATRP) of styrene and methyl methacrylate. Moderate to excellent control was achieved with dispersities as low as 1.1 for both poly(methyl methacrylate) and polystyrene. Kinetic studies showed living characteristics, and end group analysis revealed the presence of olefin-terminated polymer chains, suggesting catalytic chain transfer as a competing polymerization mechanism. Although the catalysts are not the fastest Fe ATRP mediators, they are robust and flexible. Using propylene oxide as an initiator, the complexes were active catalysts for the ring-opening polymerization of *rac*-lactide with moderate control. While the addition of propylene oxide has been reported as an efficient method of converting a metal−halide bond to a metal−alkoxide bond in situ, we show herein that this initiation mechanism can limit polymerization reproducibility and introduce an induction period.

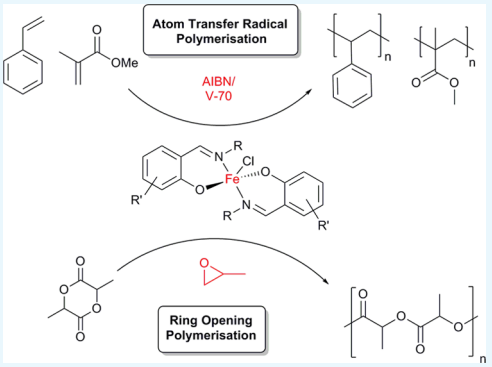

INTRODUCTION

Transition-metal complexes play an important role in the catalysis of polymerization reactions, from providing better control over the microstructure to tuning the properties of the obtained polymers.[1] Non-toxic iron is an ideal candidate to be used for this purpose as the removal of catalyst residues from polymer products is still a major challenge for food or biomedical applications.[2−4] Moreover, as Fe is the most abundant transition metal, it can maintain low costs even on industrial scales.[5,6] With multiple active oxidation states, most commonly Fe^{II} and Fe^{III}, to exploit in different catalytic processes, research in Fe-based catalysts has become an area of focus in polymer chemistry; complexes supported with a range of ligands have been characterized and applied in various types of polymerizations.[1,7−9]

Atom transfer radical polymerization (ATRP) is based on a dynamic equilibrium between the growing and the dormant polymer chains using a metal-mediated halogen-exchange process (Scheme 1). As an alternative to the typical Cu-based systems,[10] the first Fe catalysts for ATRP were pioneered by the groups of Matyjaszewski and Sawamoto, originally using $Fe^{II}X_2(PR_3)_2$ (X = Cl and Br)-type complexes.[11,12] Since then, Fe salts and complexes with a variety of ligands (including phosphines, imines, and amines) have been explored in the ATRP of vinyl monomers,[7,13,14] but interestingly the use of the ubiquitous salen ligand framework gave only limited control over the polymerization.[15] Catalysts with Fe in its more stable oxidation state can have the additional benefit of air and moisture stability that enables simple, user-friendly synthesis

Scheme 1. Mechanism of Fe-Mediated ATRP and R-ATRP

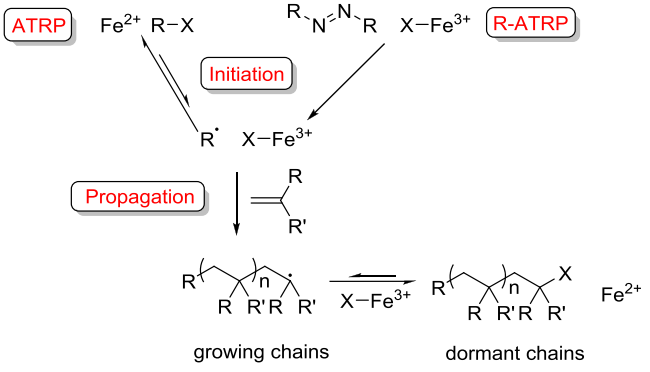

and application. These systems traditionally feature an azo initiator (such as AIBN) and proceed via a reverse ATRP (R-ATRP) mechanism (Scheme 1). The first examples of Fe-mediated R-ATRP were reported by Teyssié et al.,[16] whereas amine bisphenolate complexes of both Fe^{II} and Fe^{III} showed good control in the RP of styrene and methyl methacrylate (MMA),[17−21] through joint ATRP and organometallic-mediated radical polymerization mechanisms.[22,23]

The ring-opening polymerization (ROP) of cyclic esters, in particular the renewable cyclic diester lactide, is a burgeoning

Received: September 19, 2018
Accepted: November 22, 2018
Published: December 10, 2018

Scheme 2. Coordination−Insertion Mechanism of in Situ Fe−Alkoxide-Catalyzed Lactide Polymerization

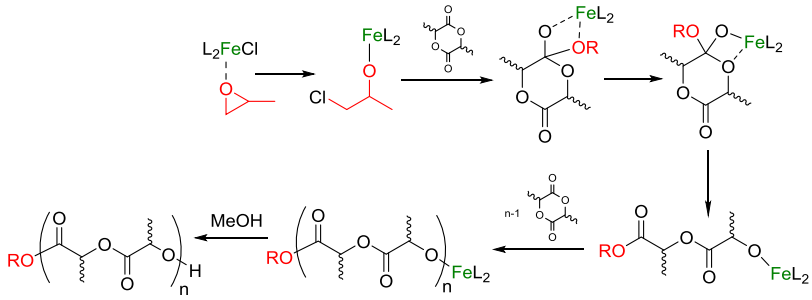

component of sustainable polymer development.[24] Industrially, poly(lactic acid) (PLA) is formed via the ROP of lactide catalyzed by Sn carboxylates. These catalysts require harsh reaction conditions, show limited control over the polymerization, and can cause toxicity problems in biomedical applications. An intense effort to develop well-defined, single site catalysts to achieve a better control over the dispersity and tacticity has led to a plethora of new catalysts for this reaction, including limited reports with some Cu complexes with relevance to ATRP.[25−28] Iron catalysts are attractive alternatives because of their low cost and biocompatibility, but surprisingly few papers report efficient Fe ROP catalyst systems.[29−36] Byers and co-workers developed a range of bis(imino)pyridine Fe alkoxide catalysts and showed that the polymerization was sensitive to both oxidation state and electron density of Fe.[9,37] Salen complexes of Fe^{II} aalso catalyzed the ROP of L-LA.[38] Following the recent trend of using propylene oxide (PO)-triggered initiations,[39−42] Duan et al. reported on the in situ generation of salen-based Fe^{III}−alkoxide catalysts for the ROP of lactide and caprolactone.[43] The proposed mechanism suggests the insertion of PO into the Fe−Cl bond to form the catalytically active Fe−alkoxide (Scheme 2). Similar to Al-based systems,[39] the addition of a massive excess (2000 equivalents) of the carcinogenic PO was required to achieve good conversions, hence greatly reducing the atom efficiency and biocompatibility of this system.

Complimentary to the well-studied tetradentate salen systems, tridentate derivatives of Schiff bases were also applied to support Fe^{III} as a polymerization catalyst.[44] Considering the paucity of studies exploring Fe complexes with bidentate phenoxyimine ligands,[45−47] we recently developed a novel family of air-stable half salen Fe^{III} chloride catalysts that showed high activity in CO_2/epoxide couplings.[48] In these reactions, the conformational flexibility of the complexes proved to be an advantage over the standard salen scaffolds. The presence of the Fe−Cl bond in these catalysts opened up the possibility of their applications in R-ATRP (Scheme 1) and ROP (Scheme 2) reactions. Half salen ligands offer the advantage of simple and modular synthesis to achieve stereoelectronically diverse properties (Figure 1). Aluminum complexes of these ligands have shown promising results in the ROP of cyclic esters,[49] including the application of monometallic Al−phenoxyimines in the ROP of γ-butyrolactone[50] and the stereocontrolled ROP of lactide.[51] Moreover, dimeric, oxygen-bridged Li, Na, and K phenoxyimine complexes were extremely active in the ROP of lactide; however, these systems exerted a lower control over molecular weights and tacticity.[52]

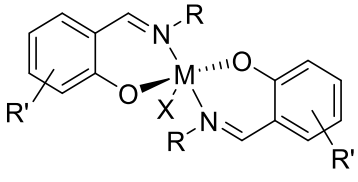

Figure 1. General structure of a bis-chelated half salen complex.

This work explores the synthesis of five bidentate phenoxyimine ligands, the corresponding novel Fe^{III} chloride complexes, and their application in polymerization catalysis. Combined with the previously reported complexes, all eight Fe−phenoxyimines were screened as mediators in the R-ATRP of styrene and MMA. Moreover, we explored the PO-triggered ROP of *rac*-lactide, including understanding the limitations of this emerging initiation strategy.

RESULTS AND DISCUSSION

Synthesis and Characterization. A series of Fe^{III} complexes were synthesized from half salen ligands, incorporating substituents with varying steric bulk [methyl or 2,6-diisopropylphenyl (DIPP)] at the imine position and peripheral Cl or ^{t}Bu substituents on the phenol moiety.[52,53] Initially, the pro-ligands were deprotonated by NaH to form the corresponding Na−phenolates. Subsequent transmetalation with anhydrous $FeCl_3$ (0.5 equiv) in tetrahydrofuran (THF) solvent at ambient temperature gave an immediate color change from yellow to dark purple, which indicated the formation of the desired L_2FeCl complexes (**C1**−**C8**). The resulting Fe complexes were isolated in moderate to high yields (45−89%) as dark purple-brown solids. As the paramagnetically shifted ^{1}H NMR spectra of the complexes provided limited information, the stoichiometry was confirmed with high-resolution mass spectrometry and elemental analysis. All eight complexes were oxygen and moisture stable, and single crystals of **C5**, **C6**, and **C8** were obtained under air via the slow evaporation of the dichloromethane (DCM) solvent (Scheme 3). X-ray diffraction studies revealed that all three complexes display a mononuclear structure with distorted trigonal bipyramidal geometries (τ = 0.94, 0.87, and 0.66 for **C5**, **C6**, and **C8**, respectively) around the pentacoordinate Fe^{III} center, using the τ factor developed by Addison et al. (where τ = 0 for perfect square pyramidal and τ = 1 for perfect trigonal bipyramidal geometries).[54] In line with the previously reported molecular structures of **C1**, **C3** and **C7**,[48] **C5** and **C8**, both feature a N−Fe−N axis which is almost linear [**C5**, N(1)−Fe(1)−N(1′), 177.44(5)°; **C8**, N(1)−Fe(1)−N(2), 169.98(6)°], with one Cl and two phenoxy-O centers occupying the equatorial positions (Figures 2 and 3). In contrast, **C6** displays an O−Fe−O axis [O(1)−Fe(1)−O(2), 173.7(2)°]. This switch in axial and equatorial occupants may

DOI: 10.1021/acsomega.8b02432
ACS Omega 2018, 3, 16945−16953

Scheme 3. Synthesis of Fe^{III} complexes C1−C8

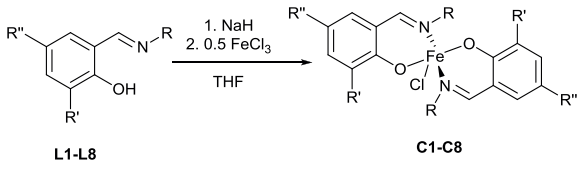

	C1[48]	C2	C3[48]	C4	C5	C6	C7[48]	C8
R	Me	DIPP	Me	DIPP	Me	DIPP	Me	Me
R'	H	H	^{t}Bu	^{t}Bu	^{t}Bu	^{t}Bu	Cl	Cl
R''	H	H	H	H	^{t}Bu	^{t}Bu	H	Cl

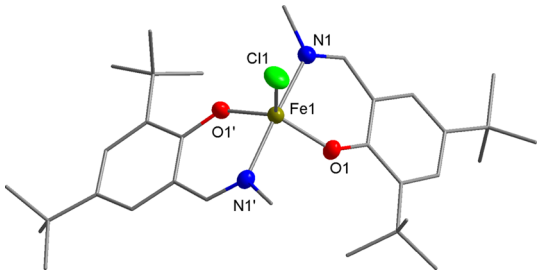

Figure 2. Molecular structure of **C5** with ellipsoids set at the 50% probability level. Hydrogen atoms have been omitted for clarity. Selected bond lengths (Å): Fe1−Cl1 2.2713(5), Fe1−O1 1.8758(9), and Fe1−N1 2.111(1). Selected bond angles (deg): O1−Fe1−Cl1 119.50(3), O1′−Fe1−O1 121.00(6), O1−Fe1−N1′ 88.46(4), O1−Fe1−N1 90.28(4), N1−Fe1−Cl1 91.28(3), and N1−Fe1−N1′ 177.44(5).

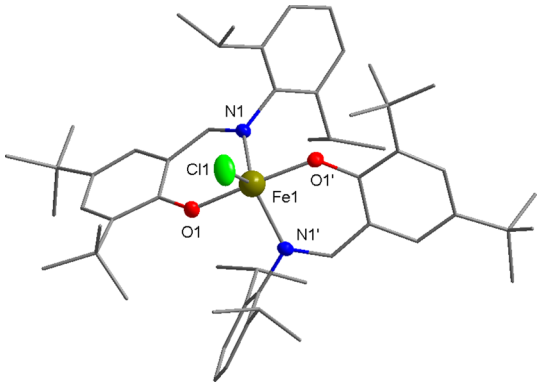

Figure 3. Molecular structure of **C6** with ellipsoids set at the 50% probability level. Hydrogen atoms have been omitted for clarity. Selected bond lengths (Å): Fe1−Cl1 2.215(2), Fe1−O1 1.921(3), and Fe1−N1 2.080(3). Selected bond angles (deg): O1−Fe1−Cl1 93.2(1), O1−Fe1−O1′ 173.7(2), O1−Fe1−N1 86.2(1), O1′−Fe1−N1 90.7(1), N1−Fe1−Cl1 119.4(1), and N1−Fe1−N1′ 121.1(2).

arise from the significant increase in steric bulk of the DIPP imine substituents. For **C5**, **C6**, and **C8** (Figure 4), the bond metrics are comparable to previously reported Fe half salen complexes,[55−59] with Fe−N bond lengths ranging from 2.101(1) to 2.111(1) Å and Fe−O bond lengths of 1.8757(9)−1.911 (1) Å. For all six structurally characterized complexes, the ancillary phenoxyimine ligands are arranged such that both nitrogen and oxygen atoms are in mutually trans positions. These geometries differ significantly from those observed with Fe^{III} salen and salalen complexes, which typically possess a square pyramidal geometry with mutually cis N and

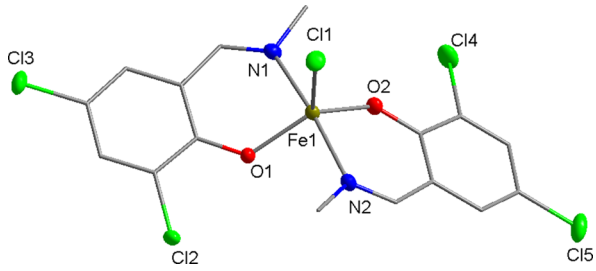

Figure 4. Molecular structure of **C8** with ellipsoids set at the 50% probability level. Hydrogen atoms have been omitted for clarity. Selected bond lengths (Å): Fe1−Cl1 2.2271(5), Fe1−O1 1.881(1), Fe1−O2 1.911(1), Fe1−N1 2.101(1), and Fe1−N2 2.104(2). Selected bond angles (deg): O1−Fe1−Cl1 114.06(4), O1−Fe1−O2 130.30(5), O1−Fe1−N1 87.91(5), O1−Fe1−N2 90.12(5), O2−Fe1−Cl1 115.64(4), O2−Fe1−N1 87.02(5), O2−Fe1−N2 86.78(5), N1−Fe1−Cl1 96.19(4), N1−Fe1−N2 169.98(6), and N2−Fe1−Cl1 93.58(4).

O ligands.[41,43] Upon the introduction of electronegative chloro substituents to the ligand scaffold, the Fe−Cl bond length is significantly shortened and strengthened, from 2.2713(5) Å for unsubstituted **C1**,[48] to 2.2517(6) Å for monochloro-substituted **C7** and to 2.2271(5) Å for *ortho*, *para*-dichloro-substituted **C8**. The magnetic moments of all eight complexes were determined via the Evans method and displayed μ_{eff} values of 4.6−5.5 B. M., which suggests that high spin Fe^{III} complexes predominate.[60]

Atom Transfer Radial Polymerization. Complexes **C1**−**C8** were screened as mediators in the R-ATRP of styrene using the standard AIBN initiator at 120 °C or an alternative azo-initiator (V-70) which 'degrades quickly to radicals at 75 °C (Table 1). As expected, the lower temperature of reaction used with V-70 leads to lower conversions and slightly narrower molecular weight distributions. Following the Fe−Cl bond strengths, the conversion increased with the Lewis acidity of the Fe center using AIBN and **C1**, **C7**, and **C8** as mediators (entries 1, 13, and 15). Surprisingly, along with providing one of the highest conversions (56%), **C8** also displayed good control over the dispersities, with $Đ$ values (1.2, entries 15 and 16) that are comparable with the best reported for Fe^{III} R-ATRP systems.[19,61] Of particular interest, catalyst **C6** was an excellent mediator using V-70, affording polystyrene with very narrow dispersity ($Đ$ = 1.05, entry 12) with matching theoretical and experimental molecular weights. This may suggest that the bulky ^{t}Bu substituents can sterically stabilize the reduced Fe^{II} derivative during the R-ATRP process. The presence of these electron-donating groups may also decrease the Lewis acidity of the metal center and therefore limit the concentration of active chains. On the contrary, when **L6** was investigated by Gibson et al. in a mono-chelated $FeLCl_2$-type complex, poor control was achieved, attributed to the relative instability of the reduced tricoordinate Fe^{II} species formed during polymerization.[44] Interestingly, **C5** with identical ^{t}Bu substituents on the phenol moiety displayed significantly lower control, which can be linked to the lack of steric hindrance and thus protection of the coordination sphere by the DIPP group on the imine. Complexes **C3** and **C4** provided a moderate degree of control ($Đ$ = 1.4−1.5), whereas **C1**, **C2**, **C5**, and **C7** were relatively poor mediators providing broad dispersities ($Đ$ > 1.5). These findings suggest that overall, the steric bulk at the imine position (Me or DIPP substituents) does not have a significant effect upon the degree of control. In some cases

DOI: 10.1021/acsomega.8b02432
ACS Omega 2018, 3, 16945−16953

Table 1. Screening of Catalysts C1−C8 in Styrene R-ATRP[a]

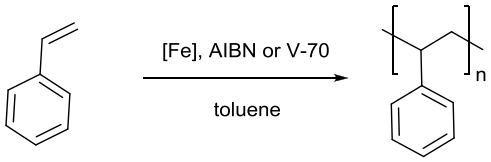

entry	complex	init.	conv. (%)	$M_{n,th}$ (Da)	M_n (Da)	$Đ$
1	**C1**	AIBN	29	3000	3800	1.7
2		V-70[b]	18	1900	3600	1.4
3	**C2**	AIBN	61	6400	11 600	1.7
4		V-70	36	3800	6800	1.5
5	**C3**	AIBN	34	3500	4000	1.5
6		V-70	24	2700	4000	1.5
7	**C4**	AIBN	40	4200	4200	1.4
8		V-70	31	3200	3300	1.5
9	**C5**	AIBN	79	8200	15 500	2.2
10		V-70	33	6800	13 800	1.8
11	**C6**	AIBN	23	2400	4200	1.4
12		V-70	25	2600	2600	1.1
13	**C7**	AIBN	45	4700	14 200	1.6
14		V-70	23	2400	6000	1.4
15	**C8**	AIBN	56	5800	10 900	1.2
16		V-70[b]	14	1500	5700	1.2

[a]Conditions: [styrene]/[Fe^{III}]/[I] = 100:1:0.6, styrene/toluene = 1:1 (v/v), 120 °C for AIBN or 75 °C for V-70, 2 h. Conversion was determined using ^{1}H NMR spectra of crude reaction mixtures. $M_{n,th\ [Fe]}$ = $[styrene]_0/[Fe] \times M(styrene) \times$ conversion. [b]Insufficient polymer was precipitated after 2 h to allow analysis; therefore, a sample precipitated after 4 h reaction time was used.

(e.g., entries 3−4 and 9−10), the number average molecular weights (M_n) were higher than the theoretical values ($M_{n,th}$), suggesting inefficient initiation.

Kinetic experiments were performed using complex **C8**, which exerted the highest control over dispersity using AIBN as the initiator. The molecular weights increased linearly with conversion, suggesting a controlled polymerization. The reaction kinetics deviated from the expected first-order dependence on monomer concentration, which may be due to the presence of competing side reactions (vide infra) (Figure 5).

To provide insight into the nature of the polymer end groups, the purified polystyrene samples were investigated by ^{1}H NMR spectroscopy. Besides the expected halide capping group (ClC*H*(Ph)CH_2 at 4.4 ppm), the presence of olefin-terminated polymer chains was also observed, as indicated by diagnostic doublets at 5.27 and 5.78 ppm (Figure 6). These

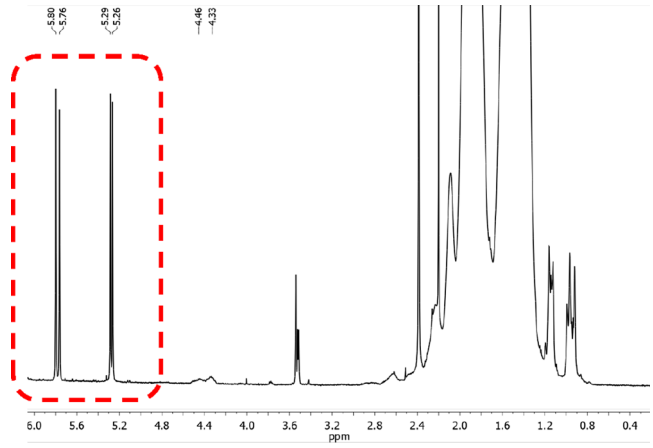

Figure 6. ^{1}H NMR spectrum ($CDCl_3$, 20 °C) showing doublet peaks of olefin-terminated polymer chains formed via CCT.

findings suggest that catalytic chain-transfer (CCT) side reactions occur, which compete with the ATRP mechanism.[18] However, molecular weights increased linearly with the conversion, as observed previously for intermediate spin α-diimine Fe complexes.[62,63]

The R-ATRP of MMA using **C1−C8** as mediators afforded polymers with M_n significantly in excess of the theoretical values ($M_{n,th}$), which is a common phenomenon using this monomer with azo initiators (AIBN and V-70).[17] Similarly to the styrene polymerizations, using **C1**, **C3**, and **C5** as mediators, the conversion increased with the presence of sterically bulky ^{t}Bu substituents on the half salen ligand scaffold (Table 2, entries 1, 5 and 9). The complexes were found to be moderate to poor mediators achieving relatively broad dispersities ($Đ$ = 1.4−2.3). The exception was the unsubstituted complex **C1**, which achieved moderate activities (28−30% conversion) while exerting good control ($Đ$ = 1.1 and 1.2 using AIBN and V-70, respectively). This observation is consistent with the general principle in normal ATRP, where the mediator must be fine-tuned so that the polymerization rate is sufficiently rapid, but not so active that radical termination dominates the reaction.[64]

Kinetic experiments using **C1** showed that the polymerization was well controlled; the molecular weight increased linearly with conversion. However, the reaction slowed down considerably, reaching a plateau at moderate conversions (Figure 7), possibly because of bimolecular termination side reactions.[7] Similarly to the polystyrene samples, ^{1}H NMR analysis revealed the presence of olefin-terminated polymer

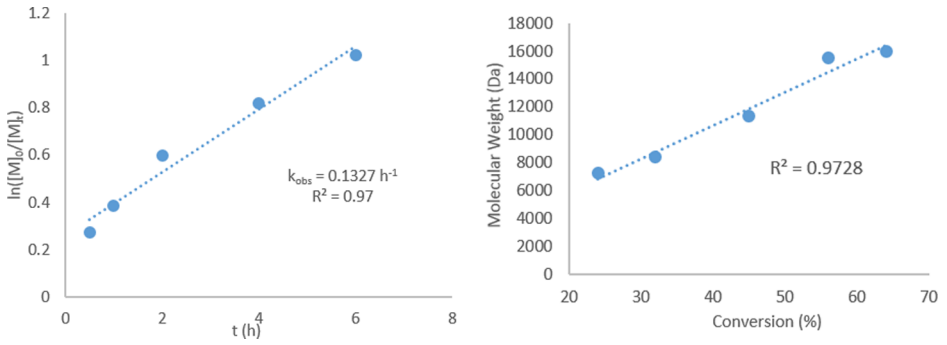

Figure 5. Kinetic plots for styrene polymerization: $\ln([M]_0/[M]_t)$ vs time (on left) and molecular weight vs conversion (right).

DOI: 10.1021/acsomega.8b02432
ACS Omega 2018, 3, 16945−16953

Table 2. Screening of Catalysts C1−C8 in MMA R-ATRP[a]

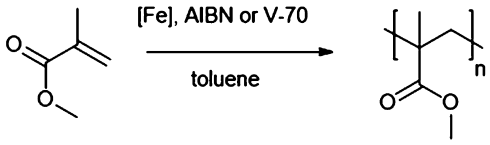

entry	complex	init.	conv. (%)	$M_{n,th}$ (Da)	M_n (Da)	$Đ$
1	**C1**	AIBN	28	2800	8400	1.1
2		V-70	30	3000	13 000	1.2
3	**C2**	AIBN	76	7600	17 000	1.8
4		V-70	66	6600	18 900	2.3
5	**C3**	AIBN	47	4700	12 700	1.6
6		V-70	24	2400	18 800	1.5
7	**C4**	AIBN	85	8500	18 400	1.4
8		V-70	68	6800	15 700	1.4
9	**C5**	AIBN	61	6100	16 700	2.2
10		V-70	54	5400	16 500	1.9
11	**C6**	AIBN	65	6500	22 800	1.4
12		V-70	62	6200	14 900	1.4
13	**C7**	AIBN	68	6800	18 900	1.7
14		V-70	62	6200	19 400	1.6
15	**C8**	AIBN	64	6400	16 100	1.8
16		V70	63	6300	16 400	1.4

[a]Conditions: [MMA]/[Fe^{III}]/[I] = 100:1:0.6, MMA/toluene = 1:1 (v/v), 120 °C for AIBN or 75 °C for V-70, 2 h. Conversion was determined using ^{1}H NMR spectra of crude reaction mixtures. $M_{n,th\ [Fe]} = [MMA]_0/[Fe] \times M(MMA) \times$ conversion.

chains (doublets at 5.50 and 6.23 ppm, Figure S14). However, the integrals of these peaks were relatively low compared to the polymer peaks, which suggested significantly less CCT than that observed for styrene.

Ring-Opening Polymerization of *rac*-Lactide. Iron catalysts remain underexplored within ring-opening polymerization reactions, yet can offer benefits in terms of low cost, biocompatibility, and air stability. Complexes **C1−C8** were therefore tested as catalysts for the ROP of lactide (LA). Most catalysts for this reaction include a metal−alkoxide initiating group, which is typically formed via the in situ conversion of a metal−alkyl group through deprotonation of an alcohol.[25] The in situ generation of metal−alkoxide catalysts through the addition of an epoxide to metal−chlorides is currently gaining momentum as an alternative initiation method (Scheme 2),[41,43] thus we tested our Fe−Cl complexes for the ROP of *rac*-LA in the presence of PO as an activator. On previously reported procedures,[41,43] we aimed to avoid the use of a large excess of PO, which would compromise the benefits of the Fe/LA system because of the toxicity of this solvent. Initial optimization of the [Fe]/PO ratio with **C8** showed that excellent conversions can be achieved with as low as 50 equivalents of PO when the reaction is carried out at 120 °C for 24 h in the toluene solvent (Table S1, entries 1−4). This modification enabled the polymerizations to be performed in airtight vials instead of autoclaves and significantly improved the overall atom efficiency. Control reactions without an Fe complex and without the addition of PO showed that both components are essential for the initiation (Table 3, entries 1 and 2). Under the optimized conditions, **C1−C8** all achieved almost complete conversion of LA (>89%), although

Table 3. ROP of *rac*-Lactide Catalyzed by Complexes C1−C8 and Propylene Oxide[a]

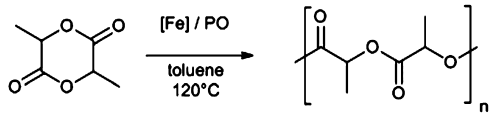

entry	complex	time (h)	conv. (%)	$M_{n,th}$ (Da)	M_n (Da)	$Đ$
1		24	0			
2[b]	**C8**	24	0			
3	**C1**	24	95	13 700	8800	1.4
4	**C2**	24	95	13 700	1500	1.7
5	**C3**	24	95	13 700	3300	1.4
6	**C4**	24	95	13 700	9000	1.6
7	**C5**	24	93	13 400	40 600	1.6
8	**C6**	24	95	13 700	2100	4.0
9	**C7**	24	93	13 400	12 600	1.8
10	**C8**	24	89	12 800	17 200	1.5
11[c]	**C1**	2	78			
12	**C2**	2	2			
13	**C3**	2	89	12 900	5500	1.1
14	**C4**	2	90	13 000	45 900	1.7
15	**C5**	2	49	7100	50 500	1.3
16	**C6**	2	91	13 100	42 200	1.5
17	**C7**	2	49	7100	22 000	1.4
18	**C8**	2	1			
19[d]	**C8**	2	90	13 000	15 900	2.1
20[d,e]	**C8**	2	89	12 800	17 200	1.5

[a]Conditions: [lactide]/[Fe]/[PO] = 100:1:50, lactide concentration in toluene = 1 M, 120 °C. Conversion was determined using ^{1}H NMR spectra of crude reaction mixtures. $M_{n,th\ [Fe]} = [lactide]_0/[Fe] \times M(lactide) \times$ conversion. [b]Reaction was carried out without the addition of PO. [c]Efforts to recover polymer were unsuccessful, indicating the formation of shorter polymer chains. [d]The Fe complex was stirred for 16 h in excess PO at room temperature prior to the addition of lactide. [e]The reaction was performed at 85 °C.

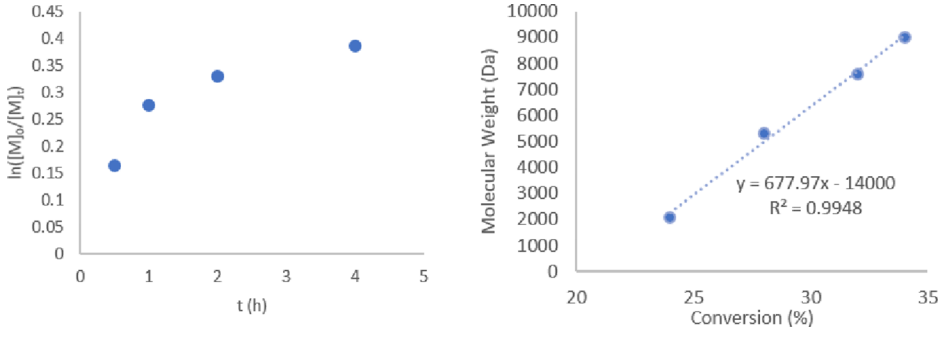

Figure 7. Kinetic plots for MMA polymerization with **C1**: $\ln([M]_0/[M]_t)$ vs time (left) and molecular weight vs conversion (right).

DOI: 10.1021/acsomega.8b02432
ACS Omega 2018, 3, 16945−16953

inconsistent molecular weights and broad dispersities indicated uncontrolled polymerizations (Table 3, entries 3−10). This was attributed to detrimental side reactions, such as intramolecular and intermolecular transesterifications, which are a commonly observed in ROP at high conversions.[25] The tacticity was investigated via homonuclear decoupled ^{1}H NMR experiments of the purified polymers, which revealed a lack of control over the tacticity with P_i values around 0.52 indicating atactic enchainments (Figure S15). To reduce the rate of undesired side reactions, the polymerization was tested under milder conditions (85 °C), affording only traces of PLA (Table S1, entry 5). Attempts to reduce the reaction time from 24 to 2 h using **C1**−**C8** led to variable conversions (Table 3, entries 11−18) with significant errors in reproducibility (Table S1, entries 6−9), suggesting that the rate-limiting step is the in situ formation of the active Fe−alkoxide catalyst. It may also suggest the presence of an induction period for the epoxide ring opening by the metal−halide, a phenomenon that was previously often observed in epoxide/CO_2 copolymerization reactions,[65−67] but may have been overlooked in the in situ formation of metal−alkoxide catalysts for ROP. The higher average molecular weights observed after 2 h of reaction time (compared to 24 h reactions) suggest the presence of extensive transesterification reactions that cleave longer polymer chains.[24] Efforts to minimize the variability through the use of a PO stock solution or a higher boiling activator (butylene oxide, bp 63 °C) were unsuccessful (Table S1, entries 6−12). The inefficient initiation observed after 2 h of reaction time using **C2**, **C5**, **C7**, and **C8** (Table 3, entries 12, 15, 17, and 18, respectively) may arise from the strength of the Fe−Cl bond. For example, the molecular structures of **C1**, **C7**, and **C8** suggest that the presence of electronegative chloro-substituents shortens and strengthens the Fe−Cl bond (vide supra). This falls in line with the conversions obtained with **C1** (78%, entry 11), **C7** (49%, entry 17), and **C8** (1%, entry 18). These results suggest that in situ initiation can lead to greater experimental variation in comparison to the use of isolated metal−alkoxide complexes. Indeed, preforming the active Fe−alkoxide species by stirring the Fe^{III}−Cl species **C8** with excess PO for 16 h, prior to the addition of LA, drastically increased the conversion from 1% (entry 18) to 90% (entry 19). Moreover, using the preformed catalyst, the reaction temperature could be lowered to 85 °C while maintaining high activity (89%, Table 3, entry 20). In accordance with initiation via epoxide opening, the matrix-assisted laser desorption ionization time-of-flight (MALDI-ToF) spectrum of the purified polymer showed a series of chains terminated by −OCH(Me)CH_2Cl and −OH groups (Figures S19 and S20). Additional polymer series bearing −OCH(Me)CH_2OH end groups were also observed, suggesting that initiation also occurs through the opening of epoxide due to the presence of trace water. In addition to the expected lactide repeat units (144 Da), the spectra also showed equally intense repeating units corresponding to a half lactide unit (72 Da), which further corroborates the prevalence of transesterification reactions. It is worth noting that poly(propylene oxide) was absent from both the MALDI-ToF and the NMR spectra of the polymer products, suggesting that no polymerization of the epoxide occurred.

CONCLUSIONS

In summary, five new monometallic pentacoordinate Fe^{III} chloride complexes were prepared based on a half salen ligand scaffold. The complexes were characterized through a combination of elemental analysis, high-resolution mass spectrometry, and in three cases, X-ray crystallography. Combined with three previously reported analogues, this series of eight complexes bearing a range of ligand substituents has been tested as mediators in the R-ATRP of styrene and MMA, achieving good to moderate control over the polymerization. The complexes have also been applied in the ROP of *rac*-lactide, generally giving >95% conversion after 24 h and showing that the in situ formation of Fe^{III}−alkoxide via epoxide opening is necessary for efficient initiation. Although this method of initiation is currently gaining momentum within ROP, some of our Fe^{III} half salen catalysts give little or no conversion after 2 h, suggesting that epoxide opening by a metal−halide may require an extreme excess of toxic epoxide (i.e., as a solvent) to achieve control. In general, these results demonstrate the versatility of simple, air-stable Fe^{III} half salen complexes and show that this abundant, inexpensive, and nontoxic metal can be a relevant alternative in polymerization catalysis.

EXPERIMENTAL SECTION

Materials and Methods. All air- and/or moisture-sensitive experiments were performed under argon atmosphere using an MBRAUN LABmaster glovebox and standard Schlenk techniques. Solvents were obtained from a solvent purification system (Innovative Technologies) consisting of columns of alumina and copper catalyst and were further degassed by freeze−pump−thaw cycles prior to use. Styrene and MMA were dried by stirring over calcium hydride, vacuum transferred, and stored at −35 °C. *rac*-Lactide was sublimed three times and stored at −35 °C. 2,2′-Azobis(4-methoxy-2,4-dimethylvaleronitrile) (V-70) was washed with methanol, dried under vacuum, and stored at −35 °C. 2,2′-Azobis(2-methylpropionitrile) (AIBN) was recrystallized from methanol, dried under vacuum, and stored at −35 °C. 2,6-Di-isopropylaniline was distilled under vacuum prior to use. *N*-Methylamine (40 m/m % in H_2O), salicylaldehyde, 3,5-dichlorosalicylaldehyde, and 3,5-di-*tert*-butylsalicylaldehyde were used as received. Gel permeation chromatography (GPC) was carried out in the HPLC grade THF solvent at a flow rate of 1 mL/min at 35 °C on a Malvern Instruments Viscotek 270 GPC Max triple detection system with 2× mixed bed styrene/DVB columns (300 × 7.5 mm). Absolute molar masses were obtained using the refractive index increment (d*n*/d*c* values) for this sample/solvent combination of 0.185 mL/g for poly(styrene),[68] 0.088 mL/g for poly(methyl methacrylate),[69] and 0.05 mL/g for PLA.[70] NMR spectra were obtained on a 500 MHz Bruker AVANCE III spectrometer. Solution magnetic moments were determined via NMR spectroscopy using Evans' method.[60] EI mass spectra were obtained on a Bruker DALTONICS micro TOF instrument operating in the positive ion electrospray mode. MALDI-ToF mass spectrometry was performed on a Bruker ultrafleXtreme MALDI-ToF spectrometer; samples were prepared with dithranol as matrix and sodium or potassium iodide as the ionization source. Elemental analyses were performed by Stephen Boyer at London Metropolitan University.

Synthetic Procedures. Pro-ligands **L1**−**L8** and complexes **C1**, **C3**, and **C7** were prepared according to previously reported literature methods.[48,53,71−73] Characterization data for **L1**,[48] **L2**,[52] **L3**,[48] **L4**,[73] **L5**,[74] **L6**,[52] and **L7**[48] were in agreement with reported values in the literature.

DOI: 10.1021/acsomega.8b02432
ACS Omega 2018, 3, 16945−16953

*Data for **L8**.* (2.90 g, 91%) ^{1}H NMR (500 MHz $CDCl_3$): δ 14.49 (s, 1H, O*H*), 8.23 (s, 1H, *H*C═N), 7.39 (d, J = 2.5 Hz, 1H, Ar*H*), 7.12 (d, J = 2.5 Hz, 1H, Ar*H*), 3.51 (d, J = 1.5 Hz, 3H, CH_3); ^{13}C NMR (126 MHz, $CDCl_3$): δ 164.9 (*C*═N), 157.8 (*C*−OH), 132.4, 128.9, 123.3, 122.2, 119.4 (Ar-*C*), 44.9 (CH_3). HRMS (EI): m/z $[M]^+$ 202.9906; calcd $[M]^+$ 202.9905. Elemental Anal. Calcd for $C_8H_7Cl_2NO$: C, 47.1; H, 3.5; N, 6.9. Found: C, 47.3; H, 3.35; N, 7.0.

General Procedure for Complexes C2, C4−C6, and C8. To a solution of pro-ligand (**L1**−**L8**) in THF solvent, 1.1 equiv of NaH was gradually added and the mixture was stirred at ambient temperature for 1 h. A solution of anhydrous $FeCl_3$ (0.5 equiv) in THF was added dropwise to afford a dark colored mixture that was stirred for a further 16 h at room temperature. Solvents were evaporated in vacuo, and the crude product was taken up in toluene solvent. The NaCl by-product was removed by filtration through celite, and the filtrate was dried in vacuo. The crude products were washed three times with hexane to afford dark purple-brown powders. Single crystals suitable for X-ray diffraction analysis were obtained via slow evaporation of DCM under air. Structures of **C5**, **C6**, and **C8** can be found under CCDC numbers 1868412−1868414.

*Data for **C2**.* (1.1 g, 52%) HRMS (EI): m/z $[M]^+$ 651.2441; calcd $[M]^+$ 651.2441. Elemental Anal. Calcd for $C_{38}H_{44}ClFeN_2O_2$: C, 70.0; H, 6.8; N, 4.3. Found: C, 70.2; H, 6.8; N, 4.4.

*Data for **C4**.* (1.1 g, 49%) HRMS (EI): m/z $[M]^+$ 763.3718; calcd $[M]^+$ 763.3693. Elemental Anal. Calcd for $C_{46}H_{60}ClFeN_2O_2$: C, 72.3; H, 7.9; N, 3.7. Found: C, 70.1; H, 7.8; N, 4.0.

*Data for **C5**.* (1.4 g, 89%) HRMS (EI): m/z $[M]^+$ 583.2790; calcd $[M]^+$ 583.2754. Elemental Anal. Calcd for $C_{32}H_{48}ClFeN_2O_2$: C, 65.8; H, 8.3; N, 4.8. Found: C, 65.9; H, 8.4; N, 4.9.

*Data for **C6**.* (1.0 g, 49%) HRMS (EI): m/z $[M]^+$ 875.5019; calcd $[M]^+$ 875.4945. Elemental Anal. Calcd for $C_{54}H_{76}ClFeN_2O_2$: C, 74.0; H, 8.7; N, 3.2. Found: C, 74.1; H, 8.8; N, 3.2.

*Data for **C8**.* (0.6 g, 45%) HRMS (EI): m/z $[M]^+$ 494.8716; calcd $[M]^+$ 494.8691. Elemental Anal. Calcd for $C_{16}H_{12}Cl_5FeN_2O_2$: C, 38.6; H, 2.4; N, 5.6. Found: C, 38.8; H, 2.5; N, 5.6.

General Procedure for the R-ATRP of Styrene and MMA. In a glovebox, the complexes (**C1**−**C8**) (24.0 μmol), monomer (100 equiv, 2.40 mmol), toluene (toluene/monomer, 1:1, v/v), and initiator (AIBN or V-70) (0.6 equiv, 14.4 μmol) were sequentially added to an airtight screwcap vial equipped with a magnetic stirrer bar. The vial was removed from the glovebox and heated to 75 or 120 °C for 2 h. The vial was subsequently cooled to room temperature, and an aliquot of the crude mixture was analyzed via ^{1}H NMR spectroscopy to determine the monomer conversion. The remainder of the reaction mixture was quenched with chloroform (approximately 1 mL), and the polymer was purified by precipitation in acidified methanol (MeOH/HCl(aq), approximately 75:1 mL). The polymer was isolated by filtration and was subsequently dried in vacuo until constant weight was achieved. Samples for GPC analysis were prepared in HPLC grade THF and filtered through a 0.22 μm pore-sized syringe filter.

General Procedure for the ROP of *rac*-Lactide. In a glovebox, complexes (**C1**−**C8**) (10.0 μmol), PO (50 equiv, 0.5 mmol), *rac*-lactide (100 equiv, 1.0 mmol), and toluene (1 mL) were added to an airtight screwcap vial equipped with a magnetic stirrer bar. The vial was transferred to the bench and heated to 120 °C in an oil bath for 24 h. The vial was subsequently cooled to room temperature, the reaction mixture was quenched with hexane, and an aliquot of the crude mixture was analyzed via ^{1}H NMR spectroscopy to determine monomer conversion. The remainder of the reaction mixture was dissolved in chloroform (approximately 1 mL), and the polymer was precipitated by the addition of the solution to cold (0 °C) acidified methanol (MeOH/HCl(aq), 75:1 mL). The polymer was then isolated by filtration and dried in vacuo until constant weight was achieved. Samples for GPC analysis were prepared in HPLC grade THF solvent and filtered through a 0.20 μm pore sized syringe filter prior to analysis.

Crystallography. Single-crystal X-ray diffraction data were collected on an Rigaku Oxford diffraction SuperNova diffractometer fitted with an Atlas CCD detector with Mo Kα radiation (λ = 0.7107 Å) or Cu Kα radiation (λ = 1.5418 Å). Crystals were mounted under Paratone on MiTeGen loops. The structures were solved by direct methods using SHELXS or SHELXT and refined by full-matrix least-squares on F^2 using SHELXL interfaced through Olex2.[75,76] Molecular graphics for all structures were generated using Diamond.

■ ASSOCIATED CONTENT

Supporting Information

The Supporting Information is available free of charge on the ACS Publications website at DOI: 10.1021/acsomega.8b02432.

GPC and HRMS data, ^{1}H NMR and MALDI spectra, and single-crystal X-ray diffraction data (PDF)

■ AUTHOR INFORMATION

Corresponding Authors

*E-mail: j.garden@ed.ac.uk (J.A.G.).
*E-mail: michael.shaver@ed.ac.uk (M.P.S.).

ORCID

Michael P. Shaver: 0000-0002-7152-6750

Notes

The authors declare no competing financial interest.

■ ACKNOWLEDGMENTS

We would like to thank Dr Benjamin Lake and Daniel Coward for useful discussions about controlled radical polymerizations. We gratefully acknowledge the University of Edinburgh and the Ramsay Memorial Trust (J.A.G.) for funding.

■ REFERENCES

(1) Chikkali, S.; Ambade, A. V.; de Bruin, B.; Shaver, M. *Metal-Catalyzed Polymerization: Fundamentals to Applications*, 1st ed.; CRC Press: Boca Raton, 2017.

(2) Platel, R.; Hodgson, L.; Williams, C. Biocompatible initiators for lactide polymerization. *Polym. Rev.* **2008**, *48*, 11−63.

(3) Tsarevsky, N. V.; Matyjaszewski, K. "Green" Atom Transfer Radical Polymerization: From Process Design to Preparation of Well-Defined Environmentally Friendly Polymeric Materials. *Chem. Rev.* **2007**, *107*, 2270−2299.

(4) Hoppe, J. O.; Agnew Marcelli, M. G.; Tainter, M. L. A review of the toxicity of iron compounds. *Am. J. Med. Sci.* **1955**, *230*, 558−571.

(5) Gopalaiah, K. Chiral iron catalysts for asymmetric synthesis. *Chem. Rev.* **2013**, *113*, 3248−3296.

(6) Jordan, T. H. Structural geology of the Earth's interior. *Proc. Natl. Acad. Sci. U.S.A.* **1979**, *76*, 4192−4200.

DOI: 10.1021/acsomega.8b02432
ACS Omega 2018, 3, 16945−16953

(7) Poli, R.; Allan, L. E. N.; Shaver, M. P. Iron-mediated reversible deactivation controlled radical polymerization. *Prog. Polym. Sci.* **2014**, *39*, 1827−1845.
(8) Raynaud, J.; Wu, J. Y.; Ritter, T. Iron-catalyzed polymerization of isoprene and other 1,3-dienes. *Angew. Chem.* **2012**, *124*, 11975−11978.
(9) Biernesser, A. B.; Li, B.; Byers, J. A. Redox-controlled polymerization of lactide catalyzed by bis(imino)pyridine iron bis(alkoxide) complexes. *J. Am. Chem. Soc.* **2013**, *135*, 16553−16560.
(10) Matyjaszewski, K.; Xia, J. Atom transfer radical polymerization. *Chem. Rev.* **2001**, *101*, 2921−2990.
(11) Ando, T.; Kamigaito, M.; Sawamoto, M. Iron(II) Chloride Complex for Living Radical Polymerization of Methyl Methacrylate. *Macromolecules* **1997**, *30*, 4507−4510.
(12) Matyjaszewski, K.; Wei, M.; Xia, J.; McDermott, N. E. Controlled/"Living" Radical Polymerization of Styrene and Methyl Methacrylate Catalyzed by Iron Complexes. *Macromolecules* **1997**, *30*, 8161−8164.
(13) Ding, M.; Jiang, X.; Peng, J.; Zhang, L.; Cheng, Z.; Zhu, X. An atom transfer radical polymerization system: catalyzed by an iron catalyst in PEG-400. *Green Chem.* **2015**, *17*, 271−278.
(14) Zhang, B.; Jiang, X.; Zhang, L.; Cheng, Z.; Zhu, X. Fe(III)-mediated ICAR ATRP in a p-xylene/PEG-200 biphasic system: facile and highly efficient separation and recycling of an iron catalyst. *Polym. Chem.* **2015**, *6*, 6616−6622.
(15) Claverie, J. Controlled living radical polymerization of styrene with iron complexes. *Res. Discl.* **1998**, 1595−1604.
(16) Moineau, G.; Dubois, P.; Jérôme, R.; Senninger, T.; Teyssié, P. Alternative Atom Transfer Radical Polymerization for MMA Using $FeCl_3$ and AIBN in the Presence of Triphenylphosphine: An Easy Way to Well-Controlled PMMA. *Macromolecules* **1998**, *31*, 545−547.
(17) Lake, B. R. M.; Shaver, M. P. Iron(ii) β-ketiminate complexes as mediators of controlled radical polymerisation. *Dalton Trans.* **2016**, *45*, 15840−15849.
(18) Coward, D. L.; Lake, B. R. M.; Shaver, M. P. Understanding Organometallic-Mediated Radical Polymerization with an Iron(II) Amine-Bis(phenolate). *Organometallics* **2017**, *36*, 3322−3328.
(19) Allan, L. E. N.; MacDonald, J. P.; Reckling, A. M.; Kozak, C. M.; Shaver, M. P. Controlled Radical Polymerization Mediated by Amine-Bis(phenolate) Iron(III) Complexes. *Macromol. Rapid Commun.* **2012**, *33*, 414−418.
(20) Schroeder, H.; Buback, M.; Shaver, M. P. Kinetics of Amine-Bis(phenolate) Iron-Mediated ATRP Up to High Pressure. *Macromolecules* **2015**, *48*, 6114−6120.
(21) Schroeder, H.; Lake, B. R. M.; Demeshko, S.; Shaver, M. P.; Buback, M. A Synthetic and Multispectroscopic Speciation Analysis of Controlled Radical Polymerization Mediated by Amine-Bis-(phenolate)iron Complexes. *Macromolecules* **2015**, *48*, 4329−4338.
(22) Lake, B. R. M.; Shaver, M. P. *Controlled Radical Polymerization: Mechanisms*; ACS, 2015; Vol. *1187*, pp 311−326.
(23) Poli, R.; Shaver, M. P. Atom transfer radical polymerization (ATRP) and organometallic mediated radical polymerization (OMRP) of styrene mediated by diaminobis(phenolato)iron(II) complexes: A DFT study. *Inorg. Chem.* **2014**, *53*, 7580−7590.
(24) Dechy-Cabaret, O.; Martin-Vaca, B.; Bourissou, D. Controlled ring-opening polymerization of lactide and glycolide. *Chem. Rev.* **2004**, *104*, 6147−6176.
(25) Stanford, M. J.; Dove, A. P. Stereocontrolled ring-opening polymerisation of lactide. *Chem. Soc. Rev.* **2010**, *39*, 486−494.
(26) MacDonald, J. P.; Shaver, M. P. *Green Polymer Chemistry: Biobased Materials and Biocatalysis*; ACS, 2015; Vol. *1192*, pp 147−167.
(27) Mandal, M.; Oppelt, K.; List, M.; Teasdale, I.; Chakraborty, D.; Monkowius, U. Copper(II) complexes with imino phenoxide ligands: synthesis, characterization, and their application as catalysts for the ring-opening polymerization of rac-lactide. *Chem. Mon.* **2016**, *147*, 1883−1892.
(28) Routaray, A.; Nath, N.; Maharana, T.; Sutar, A. k. Synthesis and Immortal ROP of L-Lactide Using Copper Complex. *J. Macromol. Sci., Part A: Pure Appl.Chem.* **2015**, *52*, 444−453.
(29) O'Keefe, B. J.; Monnier, S. M.; Hillmyer, M. A.; Tolman, W. B. Rapid and controlled polymerization of lactide by structurally characterized ferric alkoxides. *J. Am. Chem. Soc.* **2001**, *123*, 339−340.
(30) O'Keefe, B. J.; Breyfogle, L. E.; Hillmyer, M. A.; Tolman, W. B. Mechanistic Comparison of Cyclic Ester Polymerizations by Novel Iron(III)−Alkoxide Complexes: Single vs Multiple Site Catalysis. *J. Am. Chem. Soc.* **2002**, *124*, 4384−4393.
(31) Gibson, V. C.; Marshall, E. L.; Navarro-Llobet, D.; White, A. J. P.; Williams, D. J. A well-defined iron(ii) alkoxide initiator for the controlled polymerisation of lactide. *Dalton Trans.* **2002**, 4321−4322.
(32) Wang, X.; Liao, K.; Quan, D.; Wu, Q. Bulk ring-opening polymerization of lactides initiated by ferric alkoxides. *Macromolecules* **2005**, *38*, 4611−4617.
(33) Kricheldorf, H. R.; Damrau, D.-O. Polylactones, 38. Polymerization of L-lactide with Fe(II) lactate and other resorbable Fe(II) salts. *Macromol. Chem. Phys.* **1997**, *198*, 1767−1774.
(34) Stolt, M.; Södergård, A. Use of Monocarboxylic Iron Derivatives in the Ring-Opening Polymerization of L-Lactide. *Macromolecules* **1999**, *32*, 6412−6417.
(35) McGuinness, D. S.; Marshall, E. L.; Gibson, V. C.; Steed, J. W. Anionic iron(II) alkoxides as initiators for the controlled ring-opening polymerization of lactide. *J. Polym. Sci., Part A: Polym. Chem.* **2003**, *41*, 3798−3803.
(36) Kricheldorf, H. R.; Boettcher, C. Polylactones 21. Polymerization of L,L-lactide and rac-D,L-lactide with hematin and related porphyrin complexes. *Makromol. Chem.* **1993**, *194*, 463−473.
(37) Delle Chiaie, K. R.; Biernesser, A. B.; Ortuño, M. A.; Dereli, B.; Iovan, D. A.; Wilding, M. J. T.; Li, B.; Cramer, C. J.; Byers, J. A. The role of ligand redox non-innocence in ring-opening polymerization reactions catalysed by bis(imino)pyridine iron alkoxide complexes. *Dalton Trans.* **2017**, *46*, 12971−12980.
(38) Idage, B. B.; Idage, S. B.; Kasegaonkar, A. S.; Jadhav, R. V. Ring opening polymerization of dilactide using salen complex as catalyst. *Mater. Sci. Eng., B* **2010**, *168*, 193−198.
(39) Robert, C.; Schmid, T. E.; Richard, V.; Haquette, P.; Raman, S. K.; Rager, M.-N.; Gauvin, R. M.; Morin, Y.; Trivelli, X.; Guérineau, V.; del Rosal, I.; Maron, L.; Thomas, C. M. Mechanistic aspects of the polymerization of lactide using a highly efficient aluminum(III) catalytic system. *J. Am. Chem. Soc.* **2017**, *139*, 6217−6225.
(40) Anker, M.; Balasanthiran, C.; Balasanthiran, V.; Chisholm, M. H.; Jayaraj, S.; Mathieu, K.; Piromjitpong, P.; Praban, S.; Raya, B.; Simonsick, W. J. A new route for the preparation of enriched iso-polylactide from rac-lactide via a Lewis acid catalyzed ring-opening of an epoxide. *Dalton Trans.* **2017**, *46*, 5938−5945.
(41) Cozzolino, M.; Leo, V.; Tedesco, C.; Mazzeo, M.; Lamberti, M. Salen, salan and salalen iron(iii) complexes as catalysts for CO_2/epoxide reactions and ROP of cyclic esters. *Dalton Trans.* **2018**, *47*, 13229.
(42) Doherty, S.; Errington, R. J.; Housley, N.; Clegg, W. Dimeric Aluminum Chloride Complexes of N-Alkoxyalkyl-β-ketoimines: Activation with Propylene Oxide To Form Efficient Lactide Polymerization Catalysts. *Organometallics* **2004**, *23*, 2382−2388.
(43) Duan, R.; Hu, C.; Li, X.; Pang, X.; Sun, Z.; Chen, X.; Wang, X. Air-Stable Salen-Iron Complexes: Stereoselective Catalysts for Lactide and ε-Caprolactone Polymerization through in Situ Initiation. *Macromolecules* **2017**, *50*, 9188−9195.
(44) O'Reilly, R. K.; Gibson, V. C.; White, A. J. P.; Williams, D. J. Design of Highly Active Iron-Based Catalysts for Atom Transfer Radical Polymerization: Tridentate Salicylaldiminato Ligands Affording near Ideal Nernstian Behavior. *J. Am. Chem. Soc.* **2003**, *125*, 8450−8451.
(45) Silvino, A. C.; Rodrigues, A. L. C.; Resende, J. A. L. C. Synthesis, structure and application to l-lactide polymerization of a new phenoxy-imine iron(III) complex. *Inorg. Chem. Commun.* **2015**, *55*, 39−42.

DOI: 10.1021/acsomega.8b02432
ACS Omega 2018, 3, 16945−16953

(46) Al-Qaisi, F.; Genjang, N.; Nieger, M.; Repo, T. Synthesis, structure and catalytic activity of bis(phenoxyiminato)iron(III) complexes in coupling reaction of CO_2 and epoxides. *Inorg. Chim. Acta* **2016**, *442*, 81−85.
(47) van der Bergen, A.; Murray, K. S.; O'Connor, M. J.; Rehak, N.; West, B. O. N-Substituted salicylaldimine complexes of iron(III). I. Synthesis, infrared and mass spectra. *Aust. J. Chem.* **1968**, *21*, 1505−1515.
(48) Fazekas, E.; Nichol, G. S.; Shaver, M. P.; Garden, J. A. Stable Fe(III) phenoxyimines as selective and robust CO_2/epoxide coupling catalysts. *Dalton Trans.* **2018**, *47*, 13106−13112.
(49) Jianming, R.; Anguo, X.; Hongwei, W.; Hailin, Y. Review - recent development of ring-opening polymerization of cyclic esters using aluminum complexes. *Des. Monomers Polym.* **2013**, *17*, 345−355.
(50) García-Valle, F. M.; Tabernero, V.; Cuenca, T.; Mosquera, M. E. G.; Cano, J.; Milione, S. Biodegradable PHB from rac-β-butyrolactone: highly controlled ROP mediated by a pentacoordinated aluminum complex. *Organometallics* **2018**, *37*, 837.
(51) Normand, M.; Dorcet, V.; Kirillov, E.; Carpentier, J.-F. {Phenoxy-imine}aluminum versus -indium Complexes for the Immortal ROP of Lactide: Different Stereocontrol, Different Mechanisms. *Organometallics* **2013**, *32*, 1694−1709.
(52) García-Valle, F. M.; Estivill, R.; Gallegos, C.; Cuenca, T.; Mosquera, M. E. G.; Tabernero, V.; Cano, J. Metal and ligand-substituent effects in the immortal polymerization of rac-lactide with Li, Na, and K phenoxo-imine complexes. *Organometallics* **2015**, *34*, 477−487.
(53) Gotthardt, H.; Hoffmann, N. Synthese und neue [4 + 2]-Cycloadditionen von Cumarin-Abkömmlingen. *Liebigs Ann. Chem.* **1985**, *1985*, 901−912.
(54) Addison, A. W.; Rao, T. N.; Reedijk, J.; van Rijn, J.; Verschoor, G. C. Synthesis, structure, and spectroscopic properties of copper(II) compounds containing nitrogen-sulphur donor ligands; the crystal and molecular structure of aqua[1,7-bis(N-methylbenzimidazol-2′-yl)-2,6-dithiaheptane]copper(II) perchlorate. *Dalton Trans.* **1984**, 1349−1356.
(55) Becker, J. M.; Barker, J.; Clarkson, G. J.; van Gorkum, R.; Johal, G. K.; Walton, R. I.; Scott, P. Chirality and diastereoselection in the μ-oxo diiron complexes L2Fe-O-FeL2 (L = bidentate salicylaldiminato). *Dalton Trans.* **2010**, *39*, 2309−2326.
(56) Amini, M.; Arab, A.; Derakhshandeh, P. G.; Bagherzadeh, M.; Ellern, A.; Woo, L. K. A novel iron complex containing an N,O-type bidentate oxazoline ligand: Synthesis, X-ray studies, DFT calculations and catalytic activity. *Spectrochim. Acta, Part A* **2014**, *133*, 432−438.
(57) Davies, J. E.; Gatehouse, B. M. The crystal and molecular structure of chlorobis-(N-n-propylsalicylaldiminato)iron(III). *Acta Crystallogr., Sect. B: Struct. Crystallogr. Cryst. Chem.* **1972**, *28*, 3641−3645.
(58) Magurany, C. J.; Strouse, C. E. Structure and magnetism of monomeric chlorobis(N-(2-phenylethyl)salicylideniminato)iron(III), $Fe(SANE)_2Cl$. *Inorg. Chem.* **1982**, *21*, 2348−2350.
(59) Elerman, Y.; Paulus, H. A five-coordinate bis(p-bromophenylsalicylaldimino)chloroiron(III) complex. *Acta Crystallogr., Sect. C: Cryst. Struct. Commun.* **1996**, *52*, 1971−1973.
(60) Evans, D. F. 400. The determination of the paramagnetic susceptibility of substances in solution by nuclear magnetic resonance. *Chem. Commun.* **1959**, 2003−2005.
(61) Allan, L. E. N.; MacDonald, J. P.; Nichol, G. S.; Shaver, M. P. Single component iron catalysts for atom transfer and organometallic mediated radical polymerizations: mechanistic studies and reaction scope. *Macromolecules* **2014**, *47*, 1249−1257.
(62) Allan, L. E. N.; Shaver, M. P.; White, A. J. P.; Gibson, V. C. Correlation of Metal Spin-State in α-Diimine Iron Catalysts with Polymerization Mechanism. *Inorg. Chem.* **2007**, *46*, 8963−8970.
(63) Shaver, M. P.; Allan, L. E. N.; Gibson, V. C. Organometallic Intermediates in the Controlled Radical Polymerization of Styrene by α-Diimine Iron Catalysts. *Organometallics* **2007**, *26*, 4725−4730.
(64) Konkolewicz, D.; Matyjaszewski, K. *Controlled Radical Polymerization: Mechanisms*; American Chemical Society, 2015; Vol. *1187*, pp 87−103.
(65) Garden, J. A.; Saini, P. K.; Williams, C. K. Greater than the sum of its parts: A heterodinuclear polymerization catalyst. *J. Am. Chem. Soc.* **2015**, *137*, 15078−15081.
(66) Darensbourg, D. J.; Moncada, A. I. Mechanistic Insight into the Initiation Step of the Coupling Reaction of Oxetane or Epoxides and CO_2 Catalyzed by (salen)CrX Complexes. *Inorg. Chem.* **2008**, *47*, 10000−10008.
(67) Lu, X.-B.; Shi, L.; Wang, Y.-M.; Zhang, R.; Zhang, Y.-J.; Peng, X.-J.; Zhang, Z.-C.; Li, B. Design of Highly Active Binary Catalyst Systems for CO_2/Epoxide Copolymerization: Polymer Selectivity, Enantioselectivity, and Stereochemistry Control. *J. Am. Chem. Soc.* **2006**, *128*, 1664−1674.
(68) Grcev, S.; Schoenmakers, P.; Iedema, P. Determination of molecular weight and size distribution and branching characteristics of PVAc by means of size exclusion chromatography/multi-angle laser light scattering (SEC/MALLS). *Polymer* **2004**, *45*, 39−48.
(69) Min, K.; Gao, H.; Yoon, J. A.; Wu, W.; Kowalewski, T.; Matyjaszewski, K. One-pot synthesis of hairy nanoparticles by emulsion ATRP. *Macromolecules* **2009**, *42*, 1597−1603.
(70) Cairns, S. A.; Schultheiss, A.; Shaver, M. P. A broad scope of aliphatic polyesters prepared by elimination of small molecules from sustainable 1,3-dioxolan-4-ones. *Polym. Chem.* **2017**, *8*, 2990−2996.
(71) Huang, J.; Lian, B.; Qian, Y.; Zhou, W.; Chen, W.; Zheng, G. Syntheses of titanium(IV) complexes with mono-Cp and Schiff base ligands and their catalytic activities for ethylene polymerization and ethylene/1-hexene copolymerization. *Macromolecules* **2002**, *35*, 4871−4874.
(72) Cameron, P. A.; Gibson, V. C.; Redshaw, C.; Segal, J. A.; Solan, G. A.; White, A. J. P.; Williams, D. J. Synthesis and characterisation of neutral dialkylaluminium complexes stabilised by salicylaldiminato ligands, and their conversion to monoalkylaluminium cations. *Dalton Trans.* **2001**, 1472−1476.
(73) Opstal, T.; Couchez, K.; Verpoort, F. Easily accessible ring opening metathesis and atom transfer radical polymerization catalysts based on arene, norbornadiene and cyclooctadiene ruthenium complexes bearing Schiff base ligands. *Adv. Synth. Catal.* **2003**, *345*, 393−401.
(74) Safaei, E.; Kabir, M. M.; Wojtczak, A.; Jagličić, Z.; Kozakiewicz, A.; Lee, Y.-I. Synthesis, crystal structure, magnetic and redox properties of copper(II) complexes of N-alkyl(aryl) tBu-salicylaldimines. *Inorg. Chim. Acta* **2011**, *366*, 275−282.
(75) Sheldrick, G. M. Crystal structure refinement with SHELXL. *Acta Crystallogr., Sect. C: Cryst. Struct. Commun.* **2015**, *71*, 3−8.
(76) Dolomanov, O. V.; Bourhis, L. J.; Gildea, R. J.; Howard, J. A. K.; Puschmann, H. OLEX2: a complete structure solution, refinement and analysis program. *J. Appl. Crystallogr.* **2009**, *42*, 339−341.

DOI: 10.1021/acsomega.8b02432
ACS Omega 2018, 3, 16945−16953